Suppression of the Sawtooth Instability in a Storage Ring by Free-Electron Laser: An Example of Nonlinear Stabilization by Noise

R. Bartolini, G. Dattoli, L. Mezi, and A. Renieri
ENEA, Divisione Fisica Applicata, Centro Ricerche Frascati, CP 65, 00044 Frascati, Rome, Italy

M. Migliorati
Università di Roma I "La Sapienza," Dipartimento Di Energetica, Via A. Scarpa 14, 00161 Rome, Italy

M. E. Couprie and G. De Ninno
LURE, Batiment 209D, University Paris sud, BP 14, 91898 Orsay, France
and Service de Photons, Atomes et Molecules DSM/Drecam, Batiment 522, 91191 Gif-sur-Yvette, France

R. Roux
LAL, University Paris sud, 918898 Orsay, France
(Received 20 November 2000; published 10 September 2001)

The stabilization of nonlinear excitations by noise is a topic of fundamental importance in many physical problems. We discuss a genuine example within the context of storage ring-free electron laser physics, by presenting a model which allows the characterization of the system evolution and the determination of the conditions leading to the suppression of instabilities of sawtooth type. The conclusions of the model are confirmed by a comparison with experimental results on the Super Aco Storage Ring-Free Electron Laser.

DOI: 10.1103/PhysRevLett.87.134801 PACS numbers: 41.60.Cr, 29.20.Dh, 41.75.Fr

The interplay between noise (disorder) and nonlinearities is a topic of fundamental importance in a number of unsolved problems in physics [1–3]. We discuss nonlinearity-disorder interplay, within the framework of the competition between sawtooth instability (STI) and free electron laser (FEL) in storage ring (SR) based devices [4]. The multiturn interaction of the beam with the FEL radiation induces bunch lengthening and energy spread which cause the saturation of the device. The e beam may be affected by different types of instabilities, due to its interaction with the ring environment which are sources of beam quality degradation.

Longitudinal instabilities and FEL are competing nonlinear mechanisms generating noise, which manifests in an increase of the e-beam energy spread and bunch length. The competition can be traced back to the mutual feedback between the respectively induced disorders on the e beam, which may lead to the collapse of one of the two growing instabilities.

Empirical procedures based on the excitation of white noise in the radio frequency cavities of SR have been used to reduce and partially stabilize the instabilities [5].

When the e beam is passed many times inside the interaction region, the process does not preserve any memory of the FEL correlated microbunch interaction, and the long time effect on the beam of the multiturn interaction is that of a noisy contribution. We will limit our analysis to the ST manifestation of the microwave instability [6], which appears as a fast blowup in bunch length (or energy spread) followed by damping, in SRs with a relatively intense beam and a strong damping effect. The key parameter controlling the onset of the STI is

$$\delta = \frac{\langle I \rangle}{I_{\text{th}}}, \qquad I_{\text{th}} = \frac{\sqrt{2\pi}\,(E_0/e)\sigma_{\varepsilon,0}^3\alpha_c^2}{\nu_s|\frac{Z_n}{n}|}, \tag{1}$$

where $\langle I \rangle$ is the average beam current, E_0 the beam energy, n the harmonic of the revolution frequency, ν_s the synchrotron tune, (Z_n) the broadband impedance, $\sigma_{\varepsilon,0}$ the natural energy spread, and α_c the momentum compaction.

STI develops for $\delta > 1$, i.e., for large values of the e-beam average current, or for low threshold current I_{th}. We use the model equations of Ref. [7],

$$\begin{aligned} \frac{d}{dt}\alpha &= \frac{n}{T_0}2\pi\alpha_c\sigma_{\varepsilon,0}\left[\frac{\delta}{(1+\sigma^2)^{1/4}} - (1+\sigma^2)\right]\alpha, \\ \frac{d}{dt}\sigma^2 &= \left(\alpha - \frac{2}{\tau_s}\right)\sigma^2, \qquad \sigma = \frac{\sigma_i}{\sigma_{\varepsilon,0}}, \end{aligned} \tag{2}$$

where α denotes the instability growth rate, T_0 is the machine revolution period, τ_s is the damping time, and σ_i is the induced energy spread.

The right-hand side of Eqs. (2) consists of a growth contribution and a term, due to the Landau damping, which controls the instability via the diffusive or noise contribution due to the induced energy spread, ruled by the second equation. The amplitude of the instability increases with δ. By adding a white noise term to the second of Eqs. (2), we can control and even eliminate the instability.

In Fig. 1, we report the STI evolution of the induced energy spread predicted by Eq. (2), together with the experimental data from the SUPER ACO Storage Ring [8].

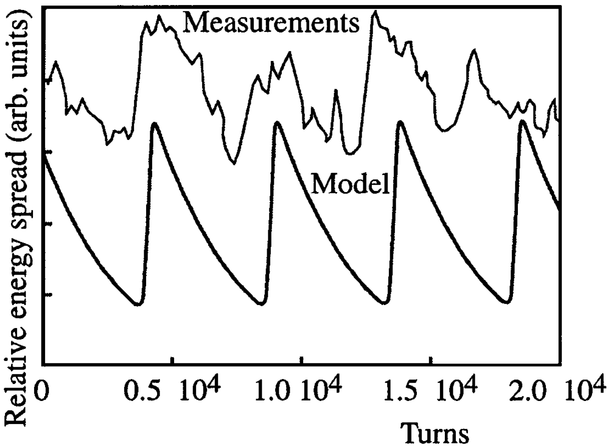

FIG. 1. Energy spread evolution predicted by Eq. (2) (curve a) and experimental results (curve b); the horizontal axis is expressed in number of machine turns; 5000 turns correspond to 1.2 ms. The other parameters are $\langle I\rangle \sim 30$ mA, $\frac{Z_n}{n} \sim 2\Omega$, $\sigma_{\varepsilon,0} \sim 6 \times 10^{-4}$, $T_0 \sim 2.4 \times 10^{-7}$ s, $E = 800$ MeV, $\tau_s \sim 9$ ms, $\nu_s \sim 6.6 \times 10^{-3}$, $\alpha_c \sim 1.4 \times 10^{-2}$, $I_{\rm th} \cong 10$ mA.

The important conclusion we can draw from the above discussion is that STI grows until the self-induced energy spread provides the necessary saturation mechanism and the damping restores the conditions for a new start-up of the instability. The mechanism we have described is similar to the SR-based FEL dynamics, whose principal saturation mechanism is associated with the self-induced multiturn energy spread [9]. We must emphasize that, in spite of the analogies, a remarkable difference between the two processes is due to the fact that FEL may reach a steady state behavior due to the saturation, while Eqs. (2) are characterized by a pseudostationary condition occurring for $\frac{d}{dt}\alpha = 0$, at values of the induced energy spread provided by

$$\sigma^* = \sqrt{\delta^{2/3} - 1}, \tag{3}$$

which is a parameter of paramount importance within the framework of FEL-STI competition. The superimposition of the FEL dynamics to Eqs. (2) is accomplished by adding the equation [7]

$$\begin{aligned} \frac{d}{dt} x(\tau, t) &= E[x(\tau + \Delta, t) G(\tau, \sigma) - r x(\tau, t)] + s(\tau), \\ r &= \frac{\eta}{0.85 g_0}, \qquad E = \frac{0.85 g_0}{T_0}, \end{aligned} \tag{4}$$

where g_0 is the FEL small signal gain and modifying the equation for the induced energy spread, by adding the contribution due to the FEL, i.e.,

$$\begin{aligned} \frac{d}{dt}\sigma^2 &= \alpha\sigma^2 - \frac{2}{\tau_s}(\sigma^2 - \bar{x}), \\ \bar{x} &= \int_{-\infty}^{\infty} x(\tau, t)\, d\tau, \end{aligned} \tag{5}$$

where x denotes the dimensionless intracavity intensity, τ is the longitudinal coordinate normalized to the electron bunch length, G is the gain function including the spectral and spatial dependence, the longitudinal distribution of the electron bunch, and the inhomogeneous degradation due to the induced energy spread, r is the ratio between cavity losses (η) and the maximum homogeneous small signal gain, S plays the role of spontaneous emission contribution, and Δ is the detuning parameter controlling the synchronism between optical and electron packet. Equation (4) is an approximate form of the FEL pulse propagation equation; it is, however, adequate to the present purposes. The definition of $x(\tau)$ in terms of physical quantities is [7]

$$x(\tau) = \frac{7.5 \times 10^{-2}}{N^2 \sigma_{\varepsilon,0}^2} \frac{\tau_s}{T_0} \frac{I(\tau)}{I_s}, \tag{6}$$

where $I(\tau)$ is the intracavity power density, and N is the number of undulator periods. I_s is the FEL saturation power density, which in practical units reads

$$\begin{aligned} I_s\left[\frac{\rm MW}{\rm cm^2}\right] &= 6.9 \times 10^2 \left(\frac{\gamma}{N}\right)^4 \frac{1}{[\lambda_u({\rm cm}) K f_b({\rm K})]^2}, \\ \gamma &= \frac{E}{m_0 c^2}. \end{aligned} \tag{7}$$

K and λ_u are the undulator strength and period length, respectively, and $f_b(\mathrm{K})$ is the Bessel factor correction. Even though (7) holds for ordinary FELs, its extension to optical klystron configurations is quite straightforward: It is sufficient to replace N by $2N(1 + d)$, where N is the number of periods of each section, and $d = \frac{N_d}{N}$ with N_d, the number of equivalent periods of the dispersive section.

The FEL-STI competition occurs according to the following scheme.

(i) If the FEL reaches an intensity sufficient to induce an energy spread larger or comparable with the threshold values σ^*, $\frac{d}{dt}\alpha = 0$, the instability is suppressed and the FEL operates without preserving any memory of its effect.

(ii) If the intracavity power is not sufficient to reach the threshold power for the suppression of the instability, the FEL may operate in a chaotic form or can be suppressed.

An example of the two regimes is given in Fig. 2, for the case of perfect synchronism. In Fig. 2a, we have reported the case of small r values; the intracavity intensity may reach large values and the FEL dominates the process providing the suppression of the instability. In Fig. 2b, we have considered a case with large r; the intracavity power is therefore low and subthreshold, the gain is not sufficient to sustain the laser growth not withstanding there is a tendency to reduce the effect of the instability.

In the case of nonperfect synchronism, the laser does not reach a steady state behavior and the interplay between FEL and STI is more interesting. The STI is indeed not turned off definitively by the onset of the laser, and we may have a revival as indicated in Fig. 3.

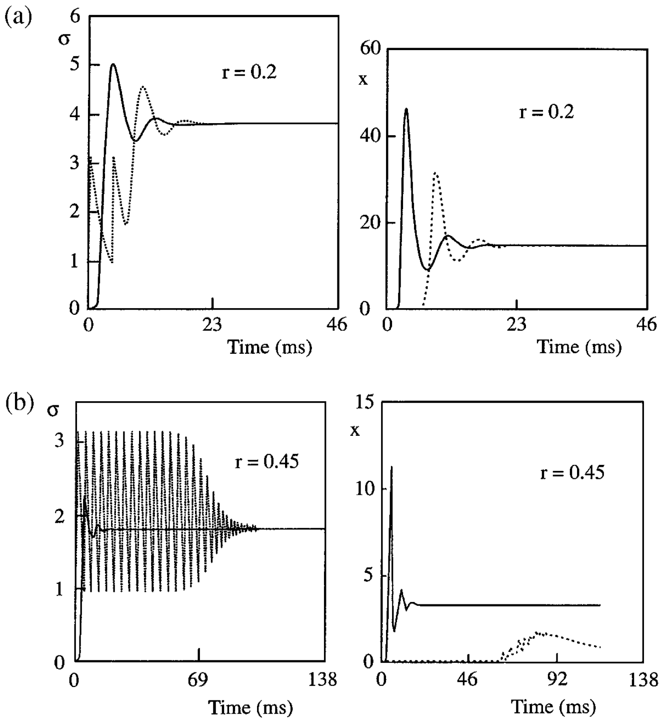

FIG. 2. STI-FEL competition $\Delta = 0$, $E = 10^4$, $\frac{n}{T_0} 2\pi \alpha_c \sigma_{\varepsilon,0} = 3 \times 10^4$, $\delta = 3$. Normalized induced energy spread σ and FEL dimensionless intracavity intensity x for (a) small cavity losses ($r = 0.2$), (b) large cavity losses ($r = 0.45$). The solid line refers to the case without STI and the dotted line corresponds to the case with STI. The small signal gain coefficient is $g = 2.5\%$.

An analogous near-subthreshold behavior has been experimentally observed at SUPER ACO as reported in Fig. 4, providing the evolution of the FEL intensity and of the electron bunch length (electron bunch and energy spread are within large limits proportional): It is evident that when the laser drops the bunch length blows up.

It is also worth noting that the threshold intracavity laser power needed to suppress the instability is, in terms of physical quantities, provided by

$$I^* = 1.673 \frac{\delta^{2/3} - 1}{g_0} \mu^2 \left(\frac{P_s}{4N} \right), \qquad \mu = 4N\sigma_{\varepsilon,0}, \quad (8)$$

where g_0 is the small signal gain coefficient, N is the number of undulator periods, and P_s is the power lost by synchrotron radiation in one machine turn. We have compared the power level of Fig. 4 with those predicted by Eq. (8) and found that they are consistent. The 20 W relevant to Fig. 4 are indeed consistent with $N \cong 120$ (including the dispersive section), $g_0 \cong 2\%$, $\sigma_{\varepsilon,0} \cong 6 \times 10^{-4}$, $\delta \sim 3$, and $P_s \cong 1$ kW.

The model we have used refers to a FEL operating in the normal configuration and the data of Fig. 4 are relevant to an optical klystron operation; the power level required to switch off the instability is, however, independent of the device configuration.

We believe that the above considerations and the comparison with the experimental results provide a physical insight into the mechanisms noise-nonlinearity interplay and confirm the conjecture put forward some years ago [10] that the onset of the FEL may suppress instabilities of longitudinal and of transverse type. We must, however, emphasize that the model we have developed, even though efficient and fast from the computational point of view, provides information on average quantities such as induced energy spread, growth rate..., but cannot provide any insight on the phase-space dynamics of the particle ensemble undergoing the combined FEL-STI interaction. We have developed a numerical analysis based on a multiparticle tracking procedure with a phenomenological impedance model [7,11]. In Fig. 5 we have reported a "tooth" evolution: (a) left bottom, (b) top, (c) half a synchrotron period from (b), (d) right bottom. The dynamics is fairly clear: The fresh beam in (a) is captured in a complicated bucket structure (b), determined by the interaction

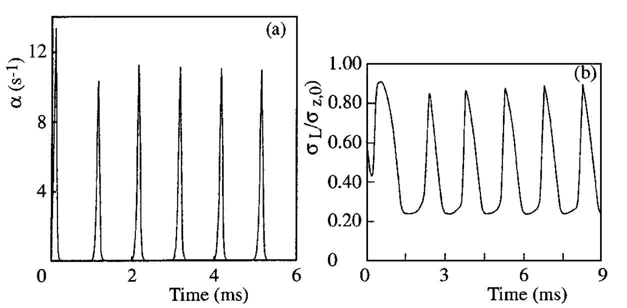

FIG. 3. Instability growth rate (a) and FEL optical pulse length normalized to the electron natural bunch length ($\sigma_{z,0} \sim 1.5$ cm) (b) vs time ($r = 0.45$, $\Delta = 0.1$, $E = 10^4$, $\frac{n}{T_0} 2\pi \alpha_c \sigma_{\varepsilon,0} = 3 \times 10^4$, $\delta = 3$). The laser does not reach a stationary behavior and the instability periodically reappears. To speed up the calculation in Figs. 2 and 3, we have assumed $\tau_s = 1.5$ ms.

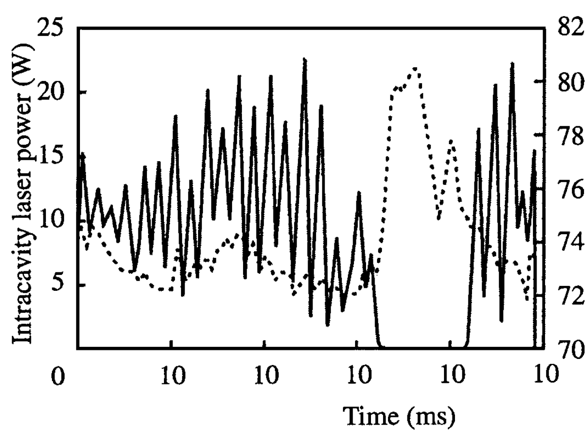

FIG. 4. Output laser intensity (solid line) and bunch length (dotted line) vs time. The data are deduced from the analysis of a double sweep streak camera image for the following experimental conditions: same parameters of Fig. 1, $r = 0.41$, $g_0 \cong 2\%$, and intracavity power 20 W.

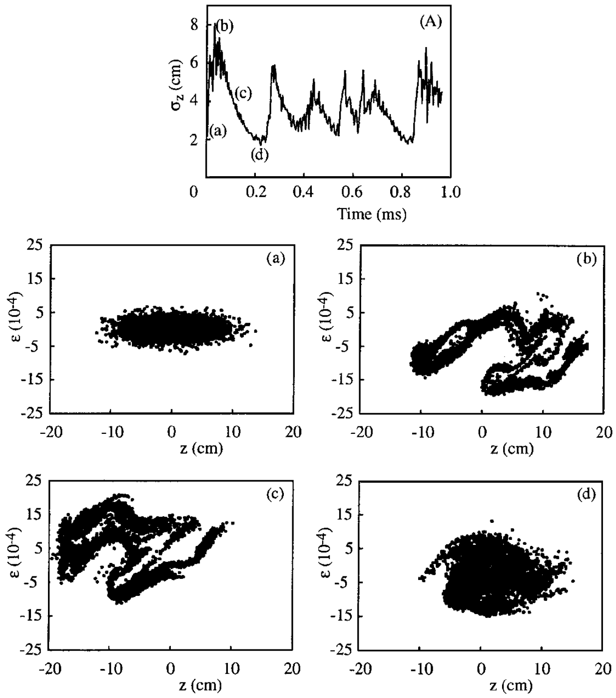

FIG. 5. e-bunch length vs time in presence of STI (A); phase-space portraits at different times on one tooth period; the configuration point c occurs after half synchrotron period from the first peak. The simulation parameters are $T_0 = 2.4 \times 10^{-7}$, $\tau_s \sim 0.12$ ms, $\langle I \rangle = 6$ mA, $\sigma_{z0} \sim 2$ cm, $\sigma_{\varepsilon,0} = 2 \times 10^{-4}$, $|z_n/n| \sim 1\ \Omega$, $\alpha_c \sim 8 \times 10^{-2}$. See text.

itself, which causes a splitting of the bunch and the consequent increase of the energy spread and bunch length. In (d) the damping has almost restored the initial conditions. In Fig. 6, we have added the FEL contribution and the phase-space dynamics is dominated by the FEL induced diffusion which smears out and makes inefficient the STI mechanism.

Anomalous bunch lengthening and energy spread may exist, without the STI manifestations, in machines characterized by low δ values and by long damping times compared to the ring turn period. In this case, the FEL instability interplay is more soft and can be treated using different methods [12].

We believe that a deeper understanding of the mechanism discussed in the paper may lead to the solution of different problems in physics and may provide efficient feedback methods.

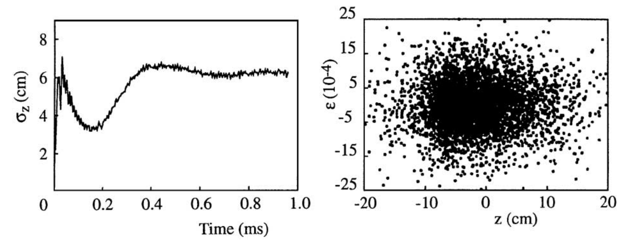

FIG. 6. Same as Fig. 5 with the inclusion of FEL interaction ($r = 0.2$); the presence of the FEL has smeared out the tooth structure and the phase space portrait is taken at large time values when the STI is switched off.

This work has been partially supported by Contract No. ERB4061PL97-0102.

[1] See, e.g., *Nonlinearity and Disorder,* edited by A. R. Bishop, D. K. Campbell, and S. Pnevmatikos (Springer-Verlag, Berlin, 1989).

[2] *Electron-Electron Interaction in Disordered Systems,* edited by A. L. Efros and M. Pollak (North-Holland, Amsterdam, 1985).

[3] K. O. Rasmussen, Yu. B. Gaididei, O. Bang, and P. L. Christiansen, Math. Comput. Simul. **40**, 339 (1996).

[4] See, e.g., K. Wille, Nucl. Instrum. Methods Phys. Res., Sect. A **393**, 18 (1997).

[5] S. Sakanaka *et al.,* Phys. Rev. ST Accel. Beams **3**, 050701 (2000).

[6] P. Krejcik *et al., Proceedings of the 1993 Particle Accelerator Conference, Washington, DC* (IEEE, New York, 1993), p. 3240. For the microwave instability in general, see J. L. Laclare, CERN 85-19 (1985), p. 377.

[7] M. Migliorati, L. Palumbo, G. Dattoli, and L. Mezi, Nucl. Instrum. Methods Phys. Res., Sect. A **497**, 134 (1999); G. Dattoli, L. Giannessi, P. L. Ottaviani, and A. Renieri, Nucl. Instrum. Methods Phys. Res., Sect. A **365**, 559 (1995).

[8] M. E. Couprie *et al.,* Nucl. Instrum. Phys. Res., Sect. A **407**, 215 (1998).

[9] F. Ciocci, G. Dattoli, A. Torre, and A. Renieri, *Insertion Devices for Synchrotron Radiation and Free Electron Laser* (World Scientific, Singapore, 2000).

[10] G. Dattoli, A. Renieri, and G. K. Voykov, Phys. Rev. E **55**, 2056 (1997).

[11] R. Baartman and M. D'yachkov, in *Proceedings of the 1995 Particle Accelerator Conference, Dallas* (IEEE, New York, 1995), Vol. 5, p. 3119.

[12] G. Dattoli, L. Mezi, M. Migliorati, and A. Renieri, Eur. Phys. J. D **6**, 375 (1999).